Early Regeneration of Thymic Progenitors in Rhesus Macaques Infected with Simian Immunodeficiency Virus

By Joanna J. Wykrzykowska,* Michael Rosenzweig,* Ronald S. Veazey,* Meredith A. Simon,* Katherine Halvorsen,‡ Ronald C. Desrosiers,* R. Paul Johnson,* and Andrew A. Lackner*

*From the *New England Regional Primate Research Center, Harvard Medical School, Southborough, Massachusetts 01772; and the ‡Department of Mathematics, Smith College, Northampton, Massachusetts 01063*

Summary

The thymus plays a critical role in the maturation and production of T lymphocytes and is a target of infection by human immunodeficiency virus (HIV) and the related simian immunodeficiency virus (SIV). Using the SIV/macaque model of AIDS, we examined the early effects of SIV on the thymus. We found that thymic infection by SIV resulted in increased apoptosis 7–14 d after infection, followed by depletion of thymocyte progenitors by day 21. A marked rebound in thymocyte progenitors occurred by day 50 and was accompanied by increased levels of cell proliferation in the thymus. Our results demonstrate a marked increase in thymic progenitor activity very early in the course of SIV infection, long before marked declines in peripheral $CD4^+$ T cell counts.

Key words: AIDS • T cell homeostasis • apoptosis • animal model • pathogenesis

The thymus plays a critical role in the maturation and production of T lymphocytes (1, 2) and is a target of infection for HIV (3–5). Infection of the thymus by HIV is thought to contribute to the depletion of $CD4^+$ T lymphocytes and the development of AIDS (6–9). This is thought to occur by induction of apoptosis and suppression of thymopoiesis, which would limit production of naive T lymphocytes (6). While the role of the thymus in T cell homeostasis in normal healthy adults is uncertain, thymic function is important for T cell regeneration after chemotherapy and presumably in conditions such as AIDS where T cells are being destroyed in large numbers (10–12). Furthermore, although T cell regeneration can occur via thymic-independent pathways, production of a diverse T cell repertoire during regeneration, a requirement for immune competence, is dependent on the thymus (13, 14). Thus, understanding how and when HIV causes thymic dysfunction is critical for understanding the pathogenesis of AIDS, for optimal timing of antiviral therapy and for attempting immune reconstitution of HIV-infected individuals.

In vivo examination of the effects of HIV on the thymus has been largely confined to the SCID-hu mouse, and to limited study of postmortem materials (3, 6, 15–18). These studies have helped elucidate the cellular targets of HIV infection and have demonstrated a direct effect of HIV on thymopoiesis. However, they have not been able to address the dynamics between peripheral T cell destruction, viral replication, host immune response and changes in the thymus, particularly early in infection. To address these issues we have used the SIV-infected macaque model of AIDS (19).

In this study we examined the effects of a pathogenic molecular clone of SIV,[1] SIVmac239, on the thymus of juvenile macaques during the first 50 d of infection. This is the time period during which plasma viral load appears to predict survival (20, 21). The thymus from these animals was examined for the presence, distribution, and immunophenotype of infected cells and for changes in T lymphocyte progenitors, cell proliferation, and apoptosis. In addition, changes in T cell subsets, viral load, and immune response were examined in the peripheral blood. Within 14 d of infection, dramatic increases in apoptosis in the thymus were observed associated with depletion of thymocyte progenitors. This was followed by a rebound in thymocyte progenitors and increased levels of cell proliferation in the thymus by 50 d after infection (dpi). This indicates that the thymus responds to the viral insult for at least a limited amount of time beginning very soon after infection, long before there are significant decreases in peripheral $CD4^+$ T cells. None of these changes were seen in animals infected with a nonpathogenic nef deletion variant of SIVmac239 (SIVmac239Δnef), despite the ability of this virus to cause significant infection of the thymus.

[1]*Abbreviations used in this paper:* dpi, days after infection; SIV, simian immunodeficiency virus.

 J. Exp. Med. © The Rockefeller University Press • 0022-1007/98/06/1767/12 $2.00
Volume 187, Number 11, June 1, 1998 1767–1778
http://www.jem.org

Materials and Methods

Animals and Viral Infections. 16 juvenile male rhesus macaques (*Macaca mulatta*) between 14 and 19 mo of age were divided randomly into two groups of 8 and were housed in accordance with standards of the American Association for Accreditation of Laboratory Animal Care. The investigators adhered to the "Guide for the Care and Use of Laboratory Animals" prepared by the Committee on Care and Use of Laboratory Animals of the Institute of Laboratory Resources, National Research Council. Before use, the animals were negative for antibodies to HIV-2, SIV, type D retrovirus, and Simian T cell leukemia virus type 1.

The two groups of animals were intravenously inoculated with equal doses (50 ng of SIV p27) of closely related pathogenic (SIVmac239) or nonpathogenic (SIVmac239Δnef) molecular clones of SIV. In addition, four healthy, age- and sex-matched rhesus monkeys were killed as normal controls. Tissues from two of the four controls were not available for flow cytometry but were used in all other analyses. SIVmac239 is the prototypic pathogenic molecular clone of SIV (22). SIVmac239Δnef is a nonpathogenic derivative of SIVmac239 with a 182-bp deletion in the nef-unique region (23).

Virus Isolation. Peripheral blood was collected for viral isolation before inoculation and at 3, 7, 14, 21, 35, and 50 d after inoculation from all animals alive at those time points. Quantitative viral cultures were performed on each blood sample as previously described (24). In brief, serial threefold dilutions were performed in duplicate beginning with 10^6 PBMCs. PBMC dilutions were cocultured with 10^5 CEMX174 cells in a volume of 1 ml. Cultures were split 1:2 twice weekly until day 21, when the cultures were assayed for virus production by ELISA for SIV p27 (Coulter, Hialeah, FL). Results are expressed as the number of SIV^+ cells/10^6 PBMCs.

SIV-specific Antibody Response and Plasma Antigenemia. SIV-specific antibodies in serum were detected by ELISA using purified whole SIVmac as previously described (25). The amount of SIV p27 per ml of plasma was determined using a commercial SIV-p27 antigen capture ELISA kit (Coulter) according to the manufacturer's recommendations. Antigen values ≥0.10 ng/ml of plasma were considered SIV antigen–positive.

Tissue Collection and Processing. Two animals from each group were killed at 7, 14, 21, and 50 dpi by intravenous injection of sodium pentobarbital. Thymus and other tissues were collected in 10% neutral buffered formalin, embedded in paraffin, sectioned at 6 μm, and stained with hematoxylin and eosin by routine histologic techniques. Adjacent sections were subjected to in situ hybridization and immunohistochemistry. Adjacent blocks of fresh tissue were collected for flow cytometry and snap-frozen for immunohistochemistry in optimum cutting temperature compound (O.C.T.; Miles Inc., Elkhart, IN), by immersion in 2-methylbutane cooled in dry ice.

Flow Cytometric Analysis of Thymocyte Progenitors. Thymic tissue was obtained at the time of death, minced into small fragments, and then digested into a single cell suspension by incubation in PBS with 0.5 mg/ml of collagenase (Sigma Chemical Co., St. Louis, MO) and 2 U/ml DNase1 (Sigma Chemical Co.) at 37°C for 30 min with frequent agitation. The cell suspension was then washed once in PBS with 2% normal mouse serum and filtered through a 70-μm nylon mesh.

Antibodies used for immunophenotyping of rhesus thymocytes included anti-CD3 (6G12; provided by J. Wong, Massachusetts General Hospital, Boston, MA; reference 26); anti-CD4 (OKT4; Ortho Diagnostic Systems Inc., Raritan, NJ); anti-CD8 (Leu-2a; Becton Dickinson, San Jose, CA); and anti-CD34 (QBend-10; Immunotech, Inc., Westbrook, ME). Cells were stained in the presence of staining media (PBS with 2% mouse serum). After antibody staining, the cells were fixed with fresh 2% paraformaldehyde. Three-color flow cytometry analysis of the cells was performed using a FACScan® with Cell Quest software (Becton Dickinson). Appropriate isotype controls were used to establish positive and negative gates. 20,000 events were collected from a live gate to exclude cellular debris.

For comparison, peripheral blood from all animals was collected in EDTA before inoculation and at 7, 14, 21, 35, and 50 dpi (from remaining animals) for analysis of lymphocyte subsets CD4 (OKT4) and CD8 (Leu-2a) using a whole blood lysis technique. Samples were analyzed as above using two-color flow cytometry.

Localization of SIV-infected Cells. Localization of infected cells was performed by immunohistochemistry for viral antigens and by in situ hybridization for viral DNA and RNA. In situ hybridization was performed on formalin-fixed paraffin-embedded sections. The DNA probe, consisting of the entire SIVmac239 genome, was labeled with digoxigenin-11-dUTP by random priming (Boehringer Mannheim, Indianapolis, IN) as previously described (24). Sections were examined microscopically and scored semiquantitatively on a scale of 0–4 as follows (Table 1): the absence of positive cells was given a score of 0; 1–5 positive cells per section a score of 1; 5–10 positive cells per 10× field a score of 2; 10–15 positive cells per 10× field a score of 3; and >15 positive cells per 10× field a score of 4. Each slide was evaluated independently by two experienced observers (M.A. Simon and A.A. Lackner) and the score presented is the mean rounded up to the next whole number.

Adjacent snap-frozen blocks of tissue were used in immunohistochemical procedures to localize virus as previously described (27, 28). In brief, tissue sections were cut at 6 μm, fixed in 2% paraformaldehyde, and immunostained using an avidin-biotin–horseradish peroxidase complex (ABC) technique with diaminobenzidine as the chromogen. The primary antibody used was Senv71.1 (SmithKline Beacham, Rixensart, Belgium), which recognizes SIV gp120. Sections were examined microscopically and scored semiquantitatively on a scale of 0–4 as described above for in situ hybridization and as shown in Table 1.

Immunophenotype of Infected Cells. To examine the immunophenotype of infected cells we performed double-label immunohistochemistry. This entailed performing immunohistochemistry for SIV gp120 as indicated above, followed by immunohistochemistry for cells of the monocyte/macrophage lineage (CD68, EBM-11; Dako Corp.) or T cells (CD2, T11; Coulter). Double labels were performed as previously described (29, 30) using Vector® blue followed by Vector® red substrates or diaminobenzidine followed by Vector® red (Vector Labs., Burlingame, CA).

Quantitation of Cell Proliferation in the Thymus. To examine cell proliferation in the thymus, 3-μm-thick sections were immunostained using the Ki67 nuclear proliferation antigen (MIB-1; Immunotech, Inc.) as previously described (31). Evaluation of cell proliferation using this antibody has been validated in several species (31–36). Diaminobenzidine was used as the chromogen and the slides were lightly counterstained with hematoxylin. Thus, all nuclei were a light blue and nuclei of proliferating cells were labeled dark brown. This difference in staining characteristics was used to determine the fraction of cells positive for Ki67 in the thymus. The fraction of positive cells was measured separately in

Table 1. *Detection and Localization of SIV Nucleic Acid and Antigen in the Thymus*

Virus	Days pi	Animal no.	In situ hybridization (cortex/medulla)*	Immuno-histochemistry
SIVmac239	7	277–93	1/2	0
		250–93	NA/NA‡	NA
	14	285–93	1/2	1
		388–93	0/1	0
	21	441–93	2/4	NA
		406–93	0/2	1
	50	434–93	1/3	3
		364–93	1/4	4
SIVmac239Δnef	7	493–93	NA/NA	0
		243–93	0/1	1
	14	251–93	0/1	1
		484–93	NA/NA	NA
	21	400–93	0/1	0
		478–93	0/1	1
	50	442–93	0/0	0
		492–93	0/0	0

* Cortex, thymic cortex; medulla, thymic medulla.
Viral antigen was found only in the medulla. Results of in situ hybridization for SIV nucleic acid and immunohistochemistry for SIV antigen were quantified as follows: no positive cells = 0; 1–5 positive cells per section = 1; 5–10 positive cells per 10× field = 2; 10–15 positive cells per 10× field = 3; >15 positive cells per 10× field = 4.
‡NA = Tissue not available for study.

the cortex and medulla in five nonoverlapping fields (527,640 μm^2) using an Olympus Vanox-S research microscope interfaced to a Quantimet 570c image analyzer (Leica, Cambridge, UK) via an Optronics DEI 750 CCD camera (Goleta, CA). The total number of cells in a field (excluding vessels, Hassals corpuscles, etc.) were traced and counted automatically according to a threshold of contrast that would detect all nuclei stained with hematoxylin or diaminobenzidine. This threshold was determined visually once for all sections. The positive cells were then counted by adjusting the threshold of contrast visually (once for all sections labeled with the same antibody) so that only cells stained with diaminobenzidine were detected. The positive cells were then traced and counted automatically. The fraction of proliferating cells was determined by dividing the total number of labeled cells in a field by the total number of cells in the same field. Each field provided a single data point for construction of box-plots and median traces (see Fig. 4).

Quantitation of Apoptosis in the Thymus. To detect apoptotic cells, sections of thymus adjacent to those used for evaluation of cell proliferation were subjected to in situ end-labeling (37) using the Apotag kit (Oncor, Inc., Gaithersburg, MD). Manufacturer's recommendations were followed except that the detection system used consisted of unlabeled polyclonal sheep antidigoxigenin antibody (Boehringer Mannheim) followed by biotinylated secondary antibody and then biotin-conjugated horseradish peroxidase complex (Vector Labs.). Diaminobenzidine served as the chromogen. This is the same detection system as used in our in situ hybridization assays and it has been previously described (24). The fraction of apoptotic cells in the cortex and medulla was then quantitated as indicated above for cell proliferation.

Quantitation of $CD4^+$ and $CD8^+$ T Cells and TIA-1 Expression in the Thymus by Morphometry. To examine absolute numbers of CD4 and CD8 single-positive T cells in the thymic medulla, 3-μm-thick sections were immunostained with monoclonal antibodies to CD4 (Nu-Th/1; Nicheri Res Institute, Tokyo, Japan) and CD8 (DK 25; Dako Corp.) as previously described (31). The fraction of cells positive for CD4 and CD8 were quantitated as described above for cell proliferation. Quantitation of CD4 and CD8 single-positive T cells was not attempted in the thymic cortex due to the high percentage of double-positive cells.

Sections of thymus (both cortex and medulla) were also immunostained with monoclonal anti-TIA-1 (Coulter). TIA-1 is a 15-kd cytotoxic granule-associated protein expressed predominantly in natural killer cells and cytotoxic T lymphocytes and a minority of cells of monocyte/macrophage lineage (38, 39). The fraction of cells positive for TIA-1 were quantitated as described above for cell proliferation.

Data Analysis. Results of the morphometric analyses were represented graphically as box-plots and median traces. Statistical significance of the data was assessed using regression analysis and nonparametric tests (Kruskal-Wallis and Mann-Whitney with Bonferroni correction) using Minitab statistical software (Minitab, Inc., State College, PA) Regression analysis was used to test the significance of the influence of viral inoculum (SIVmac239 versus SIVmac239Δnef), time (dpi), and the interaction between time and viral inoculum on the levels of apoptosis and proliferation observed in the thymic cortex and medulla.

Results

Animals and Viral Infections. To examine the early effects of SIV on the thymus, two groups of eight rhesus macaques were intravenously inoculated with equal doses (50 ng of SIV p27) of closely related pathogenic (SIVmac239) or nonpathogenic (SIVmac239Δnef) molecular clones of SIV (22, 23). Two animals from each group were killed at 7, 14, 21, and 50 dpi, the thymus was collected, and adjacent blocks of tissue were examined by histopathology, in situ hybridization, immunohistochemistry, quantitative image analysis, and flow cytometry. Peripheral blood was collected at 3, 7, 14, 21, 35, and 50 dpi and used for analysis of cell-associated viral load, plasma antigenemia, SIV-specific immune response, and lymphocyte subsets on all animals alive at those time points. Four additional healthy, age- and sex-matched rhesus monkeys were killed as normal controls.

SIV Isolation and Quantitation. Although animals inoculated with both the pathogenic molecular clone SIVmac239 ($n = 8$) and the nonpathogenic SIVmac239Δnef ($n = 8$) had virus recovered from their PBMCs within 3 d of infection, there were marked differences in viral load and plasma antigenemia (Fig. 1). As a group, animals inoculated with SIVmac239 had at least one log more virus in PBMCs than did animals inoculated with SIVmac239Δnef at every time point examined. In addition, although animals inoculated with SIVmac239 maintained high viral loads after the peak

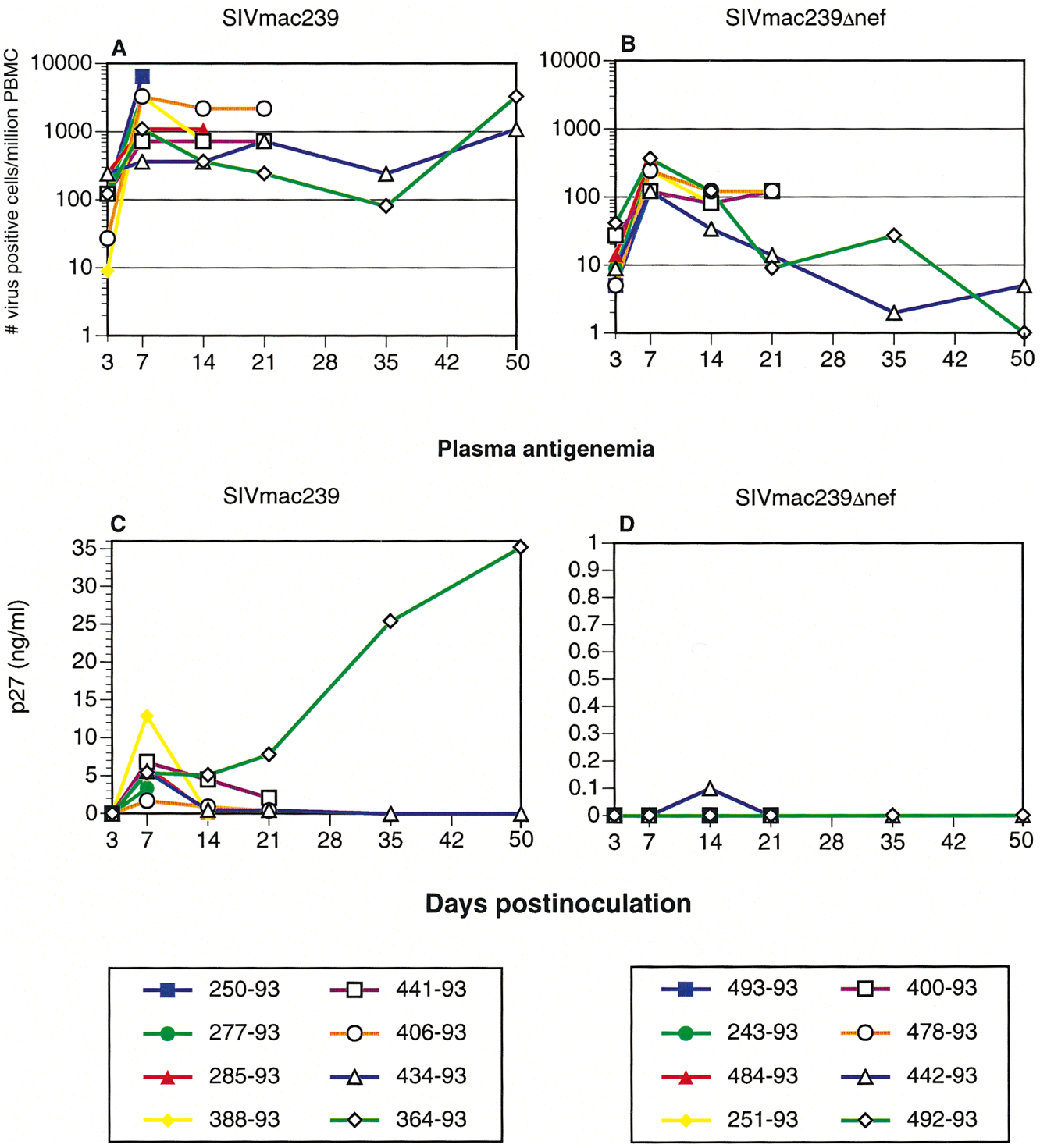

Figure 1. Quantitative virus isolation. Cell associated viral loads (*A* and *B*) and plasma antigenemia (*C* and *D*) in animals inoculated with pathogenic SIVmac239 (*A* and *C*) or nonpathogenic SIVmac239Δnef (*B* and *D*). Peak viral loads were seen at 7 dpi. Viral loads in animals infected with SIVmac239 were maintained at high levels, whereas viral loads in animals infected with SIVmac239Δnef declined to very low levels, by 50 dpi. Plasma antigenemia was transient in all animals except for 364–93, which was infected with SIVmac239. This animal demonstrated a typical "rapid progressor" profile with increasing plasma antigenemia and absence of a detectable humoral immune response.

at 7 dpi, animals inoculated with SIVmac239Δnef had a progressive decline in viral loads to the limits of detection (1 infected cell per million) by 50 dpi.

Peak plasma antigenemia in animals inoculated with SIVmac239 occurred at 7 dpi coincident with peak cell-associated viral load. Plasma antigenemia then rapidly decreased in all animals except 364–93, which demonstrated a typical "rapid progressor" profile (40, 41) with increasing

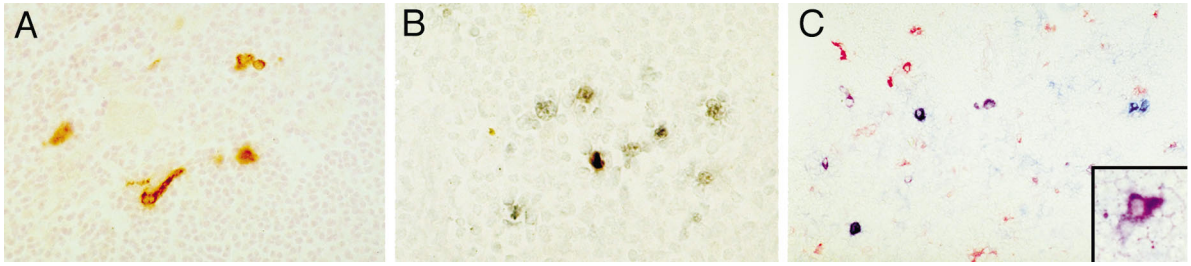

Figure 2. Localization of SIVmac239 in the thymus. Immunohistochemistry for SIV gp120 (*A*) and in situ hybridization for SIV nucleic acid (*B*) revealed many infected cells in the thymus, particularly in the medulla. The most numerous infected cells were small round to oval cells, consistent with lymphocytes. In addition, as shown in *A*, scattered cells with distinct processes were also found to be infected in the medulla. To better determine the immunophenotype of the cells with dendritic morphology, double-label immunohistochemistry was performed (*C*), combining detection of SIVgp120 (*blue*) with a marker of monocyte/macrophages (CD68, *red*). In addition to individual cells positive for CD68 only (*red*) or SIVgp120 only (*blue*), several cells are double labeled in shades of purple due to mixing of red and blue chromogens. These purple cells are SIV-infected cells of monocyte/macrophage lineage. At higher magnification (*inset*), most of the infected cells with dendritic morphology were purple, indicating that they are of monocyte/macrophage lineage. Original magnification: *A*, ×80; *B*, ×100; *C*, ×75; *inset*, ×150.

plasma antigenemia (Fig. 1 *C*) and absence of a detectable humoral immune response (data not shown). In contrast to animals inoculated with SIVmac239, only one animal inoculated with SIVmac239Δnef had detectable antigenemia. This occurred at only one time point and at the limit of detection of this assay (Fig. 1 *D*). The viral loads in animals inoculated with SIVmac239 and SIVmac239Δnef were consistent with previous observations (23, 24, 27, 42).

Infection of the Thymus Occurs during Primary Viremia. Coincident with peak viral loads at 7 dpi, virus was detected in the thymus by immunohistochemistry for SIVgp120 and by in situ hybridization for SIV nucleic acid (Table 1 and Fig. 2). Most of the infected cells detected by in situ hybridization and immunohistochemistry were present in the thymic medulla with few positive cells evident in the cortex consistent with previous observations (40, 43). Infected cells in the thymic cortex were found only in animals inoculated with SIVmac239 and only by in situ hybridization. The number of infected cells detected by in situ hybridization and immunohistochemistry in the thymus changed little over the 50-d duration of the study with consistently greater numbers of infected cells in animals inoculated with SIVmac239 than in animals inoculated with SIVmac239Δnef. By 50 dpi, virus could no longer be detected in the thymus of animals infected with SIVmac239Δnef.

Morphologically, two distinct populations of cells were infected. The most numerous were small round to oval cells, consistent with lymphocytes, and the others were scattered, considerably larger cells that often had distinct processes (dendritic morphology; see Fig. 2). To better determine the immunophenotype of the infected cells, we performed double-label immunohistochemistry combining detection of SIVgp120 with a marker of either monocyte/macrophages (CD68) or T cells (CD2). These experiments revealed that most of the infected cells in the thymic medulla with the dendritic morphology were of monocyte/macrophage lineage (Fig. 2). A subpopulation of SIVgp120$^+$ cells with dendritic morphology were negative for CD68, suggesting that they may be of a different lineage. The majority of the SIVgp120$^+$ cells, which were morphologically compatible with lymphocytes, were labeled with the T cell marker CD2 (data not shown).

Despite abundant evidence of SIV infection of the thymus, histopathologic alterations of the thymus were mild, consistent with previous observations during the first 8 wk of infection (40, 43). However, we did observe an apparent increase in the thickness of the thymic cortex in animals inoculated with SIVmac239 at 50 dpi compared with earlier time points (Fig. 3). This increase in thymic cortical thickness occurred coincident with increased cell proliferation in the cortex (see below).

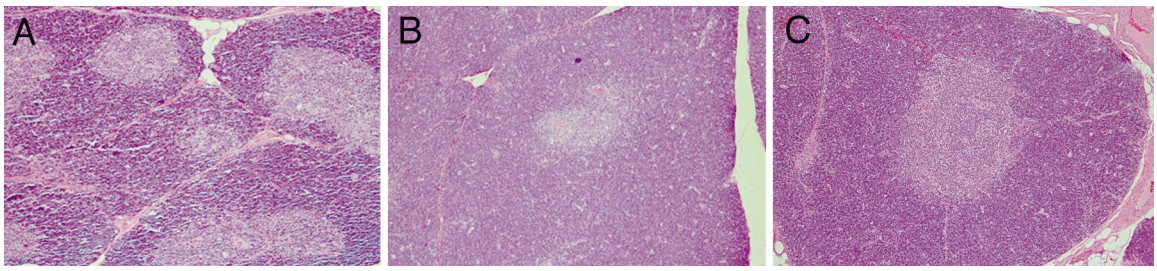

Figure 3. Morphologic alterations of the thymus. Hematoxylin and eosin stained sections of thymus from macaques infected with SIVmac239 at 14 (*A*) and 50 (*B*) dpi and from an age-matched, uninfected macaque (*C*). The photomicrographs were taken at the same original magnification (×33). As compared with the uninfected control (*C*), moderate thinning of the cortex is visible at 14 dpi (*A*), whereas at 50 dpi (*B*) the thymic cortex is at least as thick as in the uninfected control.

Alterations in Cell Proliferation and Apoptosis in the Thymus Occur Coincident with Early Peaks in Viral Load. To examine cell proliferation and apoptosis in the thymus, morphometric analyses were performed on tissue sections using immunohistochemistry for the Ki-67 nuclear proliferation antigen and TdT-mediated in situ-end labeling, respectively. The Ki-67 antigen is specific for proliferating cells found throughout the cell cycle (G1, S, G2, and M phases) and absent in resting (G0) cells (34, 35). Analyses of cell proliferation and apoptosis were performed separately for the thymic cortex and medulla (Fig. 4).

In the cortex of animals inoculated with SIVmac239, the proportion of apoptotic cells was increased by 7 dpi compared with age-matched, uninfected controls and reached a peak at 14 dpi before decreasing to normal levels at 21 and 50 dpi. This increase in apoptosis mirrored, or was slightly delayed relative to, the early peaks in cell-associated viral load and plasma antigenemia (7 dpi, Fig. 1). The levels of apoptosis in the thymic cortex of animals inoculated with SIVmac239Δnef were not statistically significantly different from those observed in uninfected controls ($P = 0.6478$). Regression analysis was used to test the significance of the influence of viral inoculum (SIVmac239 versus SIVmac239Δnef), time (dpi), and the interaction between time and viral inoculum on the observed levels of apoptosis. Both time ($P < 0.0005$) and viral inoculum ($P < 0.0005$) significantly influenced the levels of apoptosis. The interaction of time and viral inoculum also significantly ($P < 0.0005$) influenced the levels of apoptosis. The interaction between time and viral inoculum can be seen in Fig. 4. The increase in apoptosis cannot be attributed to a stress response because all animals were housed and handled

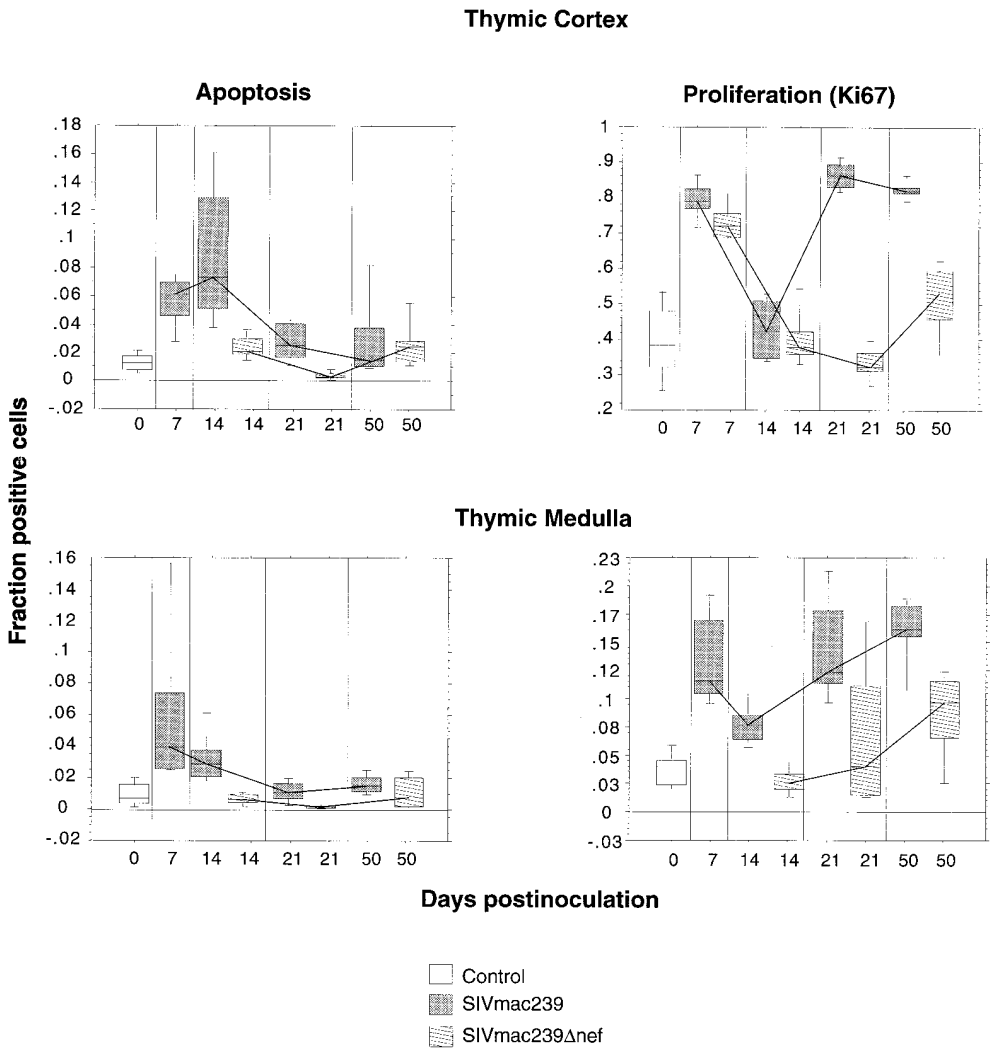

Figure 4. Apoptosis and cellular proliferation in the thymus during SIV infection. Alterations in cell proliferation and apoptosis in the thymic cortex and medulla were examined by morphometry in sections of thymus from animals infected with pathogenic SIVmac239 or nonpathogenic SIVmac239Δnef and compared with four uninfected control animals. Results are illustrated as box-plots and median traces. The box plots are based on 10 observations (20 for the controls), 5 from each animal. Each box-plot represents pooled data from two animals infected with the same virus or four uninfected age-matched controls. To examine cell proliferation, the fraction of cells positive for the Ki67 nuclear proliferation antigen were measured separately in the cortex and medulla using a Quantimet 570c image analyzer. The fraction of cells undergoing apoptosis was similarly determined after sections were subjected to in situ end labeling using the Apotag kit. The most dramatic changes occurred in the thymic cortex of animals infected with SIVmac239, where there was an increase in apoptosis at 14 dpi followed by an increase in proliferation at 21–50 dpi. Note that the scale of the Y axis for proliferation in the thymic cortex goes to 1, indicating that at 21 and 50 dpi nearly all of the cells in the cortex were proliferating. With the exception of an early increase in proliferation in the cortex, animals infected with SIVmac239Δnef showed no significant differences from the uninfected control group.

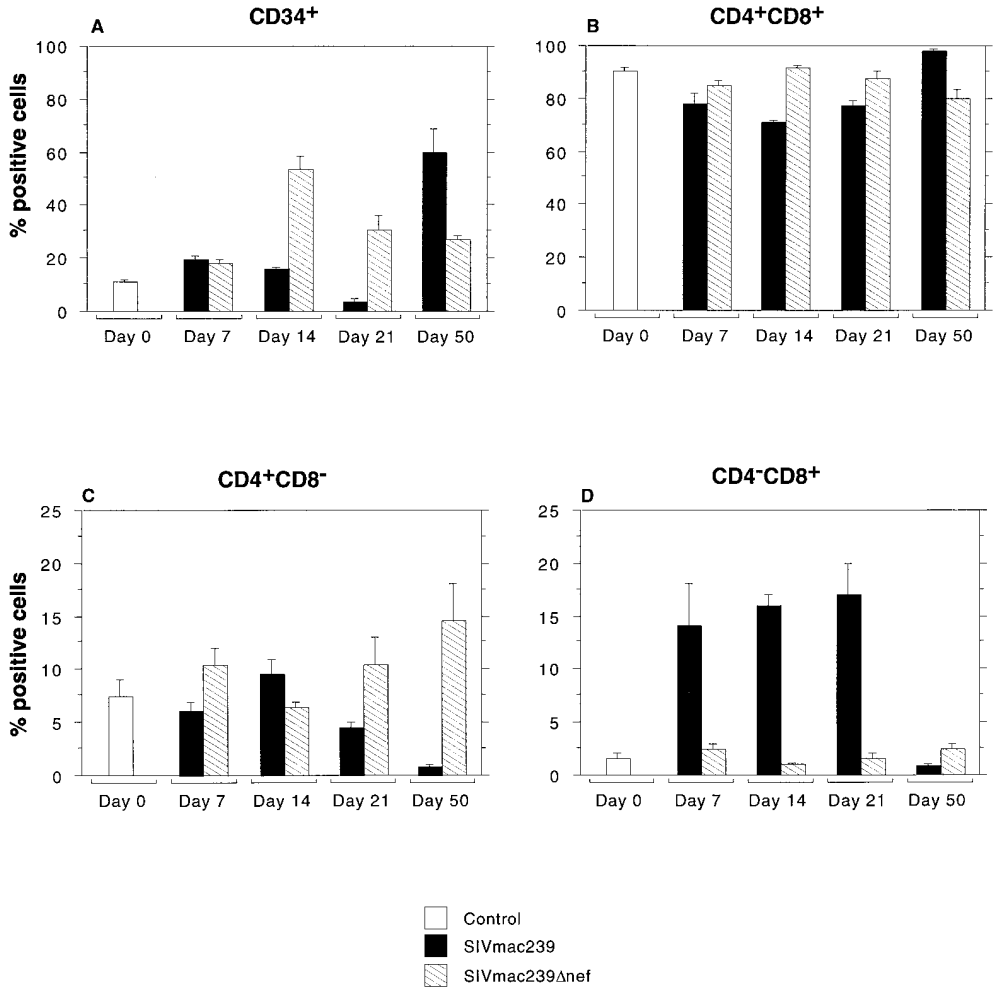

Figure 5. T lymphocyte progenitors in the thymus. Flow cytometric analysis of thymocyte progenitors was performed on single cell suspensions of thymus collected at the time of euthanasia. Three-color flow cytometry was performed with antibodies to surface CD3, CD4, CD8, and CD34. The figure shows the proportion of positive cells for controls and for animals infected with SIVmac239 or SIVmac239Δnef at each time point. Bar heights indicate mean percentage of positive cells and whiskers above bars show one SEM. Animals infected with SIVmac239 had a decrease in both $CD34^+$ and $CD4^+$ $CD8^+$ populations through d 21 followed by a dramatic rebound by 50 dpi. Marked changes in CD4 and CD8 single-positive cells were also seen in the thymus in animals infected with SIVmac239 including a striking increase in $CD4^-CD8^+$ cells through d 21 and a marked decrease in the relative percentage of both CD4 and CD8 single-positive cells by d 50. The latter is likely due to the relative increase in the percentage of $CD34^+$ and $CD4^+CD8^+$ T cell progenitors. Animals infected with SIVmac239Δnef showed few significant changes with the exception of an increase in $CD34^+$ cells at 14 dpi.

identically. Furthermore, serum cortisol levels showed no significant differences among the groups or over time (data not shown).

Proliferation in the cortex was significantly elevated in all SIV-infected animals by 7 dpi and then rapidly decreased to the normal range. This early increase in proliferation occurred during peak cell-associated viral load and plasma antigenemia. The level of proliferation in animals inoculated with SIVmac239 then rapidly increased between 14 and 21 dpi and stayed at a high level. In contrast, proliferation in the thymic cortex of animals inoculated with SIVmac239Δnef, which had progressively less virus over time, remained low. Similar to apoptosis, regression analysis showed that proliferation in the cortex was significantly influenced by the viral inoculum ($P = 0.010$), time after infection ($P < 0.0005$), and the interaction between time and inoculum ($P < 0.0005$).

Levels of apoptosis and cell proliferation in the thymic medulla (Fig. 4) mirrored the findings in the thymic cortex but were more subtle with a consistently smaller fraction of cells positive for each measure. As in the thymic cortex, no significant differences in apoptosis were observed between animals inoculated with SIVmac239Δnef and controls. In addition, as in the thymic cortex, regression analysis showed a significant influence of viral inoculum and time after infection on levels of apoptosis (virus, $P < 0.0005$; time, $P < 0.0005$) and cell proliferation (virus, $P = 0.004$; time, $P < 0.0005$).

Consistent with the observed increase in the fraction of proliferating cells detected by image analysis, we also observed an increase in forward light scatter by flow cytometry in thymocytes obtained from animals infected with SIVmac239 at 21 and 50 dpi as compared with uninfected controls or animals infected with SIVmac239Δnef (data not shown). A subjective increase in the numbers of mitotic figures in the thymic cortex was also observed by routine histology.

In addition to the changes that occurred over time, statistically significant differences were found between the pooled group of SIVmac239-infected animals ($n = 8$) and age-matched, uninfected controls ($n = 4$) with respect to proliferation or apoptosis in the thymic cortex or medulla ($P < 0.001$ for all measures). Furthermore, highly significant differences were also found between the pooled group of SIVmac239-infected animals ($n = 8$) and animals infected with SIVmac239Δnef ($n = 8$) with respect to these same measures ($P < 0.0001$ for proliferation or apoptosis in the thymic cortex or medulla). In contrast, no significant differences were found between the control group ($n = 4$)

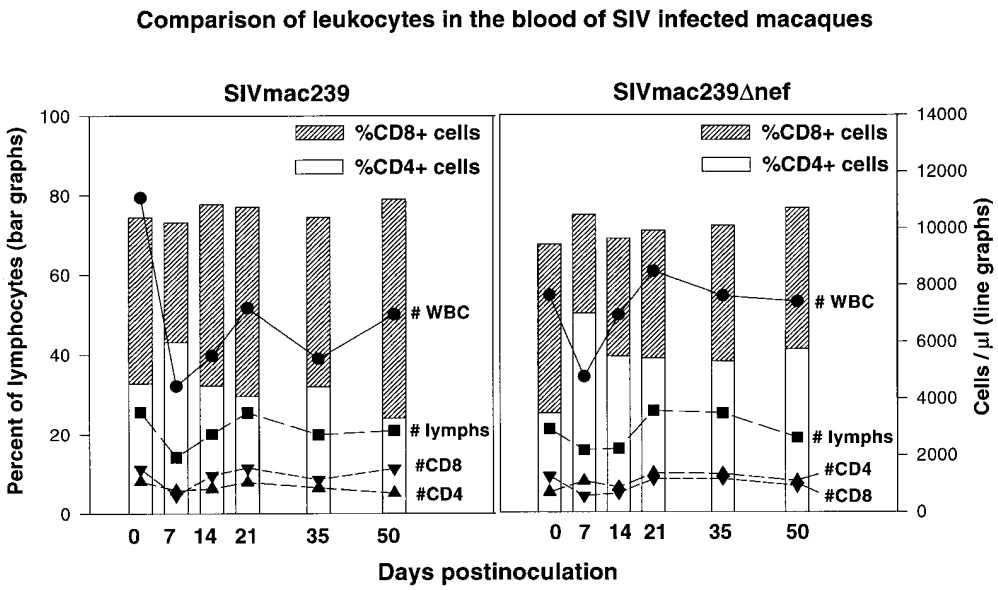

Figure 6. Flow cytometric analysis of peripheral blood leukocytes in animals before and after infection with SIVmac239 or SIVmac239Δnef. Animals inoculated with SIVmac239 show a mild decline in CD4/CD8 ratio associated with a minimal decrease in $CD4^+$ T cells and a small increase in CD8 cells. No significant alterations in $CD4^+$ or $CD8^+$ T cell numbers, percentages, or CD4/CD8 ratios were observed in animals inoculated with SIVmac239Δnef.

and the group infected with SIVmac239Δnef ($n = 8$) for either proliferation or apoptosis in the thymic cortex or medulla ($P \geq 0.1502$ for all measures).

To assess a possible role of T cell–mediated cytotoxicity in the increase in apoptosis, sections of thymus adjacent to those used for quantitation of apoptosis and proliferation were immunostained for TIA-1, and the proportion of positively stained cells was determined by morphometry. TIA-1 is a cytotoxic granule-associated protein found predominantly in natural killer cells and cytotoxic T lymphocytes and a minority of cells of the monocyte/macrophage lineage (38, 39). No change in the fraction of TIA-1 positive cells was observed over time or among the groups in either the thymic cortex or medulla.

Changes in Thymocyte Progenitors Correlate with Changes in Cell Proliferation and Apoptosis. Samples of thymus adjacent to those used for viral localization and quantitation of cell proliferation and apoptosis were analyzed by multiparameter flow cytometry using antibodies specific for CD3, 4, 8, and 34. The relative percentage of $CD34^+$ progenitor cells, and to a lesser extent $CD4^+CD8^+$ cells, decreased through 21 dpi in animals inoculated with SIVmac239, as shown in Fig. 5. The decrease in thymic progenitors occurred immediately after peak levels of apoptosis in the thymus (Fig. 4). By 50 dpi, a marked rebound in the percentage of $CD34^+$ progenitors was seen that occurred coincident with a marked increase in cell proliferation in the thymic cortex (Fig. 4).

Significant alterations in the relative percentage of CD4 and CD8 single-positive lymphocytes were also observed in SIVmac239-infected animals (Fig. 5). Most striking was the increase in $CD8^+CD4^-$ cells through 21 dpi and the marked decrease in both CD4 and CD8 single-positive cells by 50 dpi, which is probably due, at least in part, to the relative increase in the $CD4^+CD8^+$ and $CD34^+$ cells, resulting in a relative decrease of single-positive cells. At the time of $CD34^+$ rebound in the thymus, a high percentage of the $CD34^+$ cells also coexpressed CD4 and CD8 (data not shown) as has been previously described in humans (44). Despite these significant shifts in the percentages of $CD34^+$, $CD4^+CD8^+$, and CD4 and CD8 single-positive cells, the percentages and absolute numbers of CD4 and CD8 cells in the peripheral blood of these same animals had changed little (Fig. 6).

In contrast to animals inoculated with SIVmac239, animals inoculated with SIVmac239Δnef had minimal changes in the relative percentages of all subsets of cells examined in the thymus, which agrees with the lack of significant changes in cell proliferation and apoptosis observed by morphometric analyses (Figs. 4 and 5). The one exception was an increase in the percentage of $CD34^+$ cells at 14 dpi (Fig. 5). This occurred immediately after a transient increase in proliferation in the thymic cortex at 7 dpi (Fig. 4), which also coincided with peak viremia.

To further examine the influence of the relative increase in $CD4^+CD8^+$ and $CD34^+$ cells on percentages of single-positive cells, we performed morphometric analyses of the proportion of cells positive for CD4 or CD8 by immunohistochemistry in the thymic medulla. These morphometric data did not show a statistically significant decrease in CD4 or CD8 cells, although there was a trend toward a smaller proportion of $CD4^+$ cells with increasing time in animals infected with SIVmac239 (data not shown). Thus, the decrease in the percentage of CD4 and CD8 single-positive cells observed in the thymus by flow cytometry would appear to be due to the increase in thymic progenitors ($CD4^+CD8^+$ and $CD34^+$). However, this analysis was limited to the thymic medulla due to the high percentage of $CD4^+CD8^+$ cells in the thymic cortex.

Discussion

Our study demonstrates that the thymus is not only a primary target of SIV infection but that significant changes

in cell proliferation, apoptosis, and percentages of T cell precursors occur very early in the thymus coincident with the presence of infected cells and primary viremia. Of particular interest was the marked rebound in T cell progenitors ($CD34^+$ and $CD4^+CD8^+$, Fig. 5) accompanied by increased levels of cell proliferation in the thymus (Fig. 4). This occurred in the face of persistent high-level virus replication (Fig. 1 and Table 1) and provides strong evidence that the thymus has significant regenerative capacity through at least the first 7 wk of infection. However, by 24 wk of infection, morphologic evidence of severe thymic damage is evident in most SIV-infected animals, but can also occur earlier in rapid progressors as previously described (40, 43). Similarly, severe thymic damage is a consistent feature of advanced HIV infection, and a more rapid progression to AIDS has been observed in HIV-infected children with evidence of early thymic dysfunction (45). Thus the regenerative capacity of the thymus is clearly limited in the face of HIV infection.

The length of this apparent early window of time during which the thymus can regenerate is of increasing importance with the advent of potent multidrug therapies for HIV. These multidrug therapies have been remarkably successful in decreasing viral loads and partially restoring or maintaining $CD4^+$ T cell numbers. However, our data imply that if combination drug therapy for HIV is not started early enough in infection, T cell regeneration will occur with minimal help of the thymus, resulting in a limited T cell repertoire. Indeed, Connors et al. (46) have recently shown that disruptions of the $CD4^+$ T cell repertoire associated with HIV infection are not initially corrected by combination antiviral or immune-based therapies. Moreover, the initial rebound of $CD4^+$ T cells after potent combination antiretroviral therapy appears to consist primarily of memory cells. However, increases in naive $CD4^+$ T cells may occur after prolonged therapy or in patients who have maintained naive cells (46, 47). Finally, there are several recent reports of patients on multidrug therapies with relatively high CD4 counts developing opportunistic infections (48, 49). These findings, in conjunction with those of Mackall et al. (13) further support the concept that a functional thymus is critical for regeneration of a diverse T cell repertoire in HIV-infected patients.

The increased apoptosis in the thymus and initial depletion of thymocyte progenitors in animals infected with SIVmac239 occurred soon after peak viral loads in the blood and coincident with localization of virus to the thymus, suggesting a causal relationship. However, it is not clear whether these changes are due to direct effects, such as viral infection of thymic progenitors and loss of infected cells due to the cytopathic effects of the virus, or indirect effects via the induction of programmed cell death in "bystander cells." Studies using the HIV-infected SCID-hu mouse model have also implicated at least two mechanisms: induction of programmed cell death in uninfected thymocytes and interruption of thymopoiesis by direct infection and destruction of thymocyte progenitors (6, 15, 16). Furthermore, the immune response is likely to play a role in these processes via the action of natural killer cells and cytotoxic lymphocytes directed at infected cells. However, no increase in the proportion of cells expressing TIA-1 was found in the thymus, which would be expected if increased numbers of cytotoxic lymphocytes or natural killer cells were present. However, expression of TIA-1 is not antigen-specific, and so although the fraction of TIA-1–expressing cells did not increase, the number of SIV-specific cytotoxic lymphocytes may have increased.

For a direct effect, virus would presumably need to infect immature thymocytes that reside primarily in the cortex. Although viral infection of the thymic cortex could be demonstrated by in situ hybridization, all of the cells detected by immunohistochemistry, and most of the cells detected by in situ hybridization, were in the thymic medulla. Thus, although virus was present in the cortex where the most dramatic morphometric and immunophenotypic changes were observed, these alterations occurred in the absence of detectable viral protein. This would suggest that both direct and indirect mechanisms of thymocyte depletion are involved.

These findings may have important implications for T cell homeostasis. Despite the dramatic shifts in apoptosis, cell proliferation, and percentages of $CD34^+$, $CD4^+CD8^+$, and CD4 and CD8 single-positive cells in the thymus, the percentages and absolute numbers of CD4 and CD8 cells in the peripheral blood of these same animals changed little over the 50-d period (Fig. 6). This suggests that the thymus responds very rapidly to increased demand for T cells in the periphery by increasing production (increased cell proliferation, and thymocyte progenitors by 50 dpi) of mature T cells in order to maintain T cell numbers in the peripheral blood. Moreover, evidence of increased demand for T cells comes from recent studies using in vivo bromodeoxyuridine labeling by Rosenzweig et al., who have shown that, compared with normal macaques, rates of T cell turnover in chronically SIV-infected macaques are increased two- to threefold for both $CD4^+$ and $CD8^+$ T cells (50). This "opening of the tap" to compensate for increased T cell turnover (the open drain) in HIV infection has been previously suggested by Ho et al. (12). In future studies it will be important to determine how long the thymus can continue to contribute to T cell regeneration beyond the 50 d of this study.

In contrast to animals infected with SIVmac239, animals inoculated with the same dose of the nonpathogenic nef deletion derivative of SIVmac239, SIVmac239Δnef, caused few if any detectable changes in cell proliferation, apoptosis, or thymocyte progenitors despite the presence of infected cells in the thymus. Although the differences may reflect the higher viral loads in SIVmac239-infected animals, at the peak of viremia (7 dpi) differences were not as pronounced between the groups (~10-fold difference) as at latter time points (~1,000-fold difference). Moreover, individual animals in each group had equivalent viral loads (e.g., 434–93 infected with SIVmac239 and 492–93 infected with SIVmac239Δnef each had 365 viral infected cells/10^6 PBMCs at 7 dpi). Thus, these differences may be attributed, at least in part, to the presence of a functional *nef*

gene. This could occur via the effects of nef on signal transduction and activation of T cells (51). Thymocyte maturation involves a complex series of developmental stages all of which involve signal transduction from the cell surface to the nucleus. If nef is able to alter signal transduction in immature thymocytes, as it apparently does in mature T cells, it could result in inappropriate cell activation and programmed cell death.

This study shows clear and dramatic effects of SIV infection on the thymus. After an initial increase in apoptosis and loss of thymocyte progenitors, a marked rebound in cell proliferation and regeneration of T cell progenitors was seen. The duration of this rebound and the cellular mechanisms responsible for increased cell death in the thymus of SIV-infected macaques are important areas for future study.

We thank Dr. Prabhat Sehgal and the animal care staff at the New England Regional Primate Research Center for their excellent care of the animals and Dr. Vito Sasseville for careful reading of the manuscript. We also thank Sue Czajak, Douglas Marks, Jr., and Douglas Pauley for technical assistance.

This work was supported by Public Health Service grants NS-30769, AI-38559, AI-39423, RR-07000, and RR-00168. A.A. Lackner is the recipient of an Elizabeth Glaser Scientist Award.

Address correspondence to Andrew A. Lackner, New England Regional Primate Research Center, Harvard Medical School, 1 Pine Hill Dr., PO Box 9102, Southborough, MA 01772. Phone: 508-624-8018; Fax: 508-624-8181; E mail: alackner@warren.med.harvard.edu

Received for publication 10 December 1997 and in revised form 11 March 1998.

References

1. Spits, H., L.L. Lanier, and J.H. Phillips. 1995. Development of human T and natural killer cells. *Blood*. 85:2654–2670.
2. Haynes, B.F., S.M. Denning, P.T. Le, and K.H. Singer. 1990. Human intrathymic T cell differentiation. *Semin. Immunol*. 2:67–77.
3. Schuurman, H.J., W.J.A. Krone, R. Broekhuizen, J.V. Baarlen, P. vanVeen, A.L. Goldstein, J. Huber, and J. Goudsmit. 1989. The thymus in acquired immune deficiency syndrome: comparison with other types of immunodeficiency disease and presence of components of human immunodeficiency virus type 1. *Am. J. Pathol*. 134:1329–1334.
4. Burke, A.P., D. Anderson, W. Benson, R. Turnicky, P. Mannan, Y.H. Liang, J. Smialek, and R. Virmani. 1995. Localization of human immunodeficiency virus 1 RNA in thymic tissues from asymptomatic drug addicts. *Arch. Pathol. Lab. Med*. 119:36–41.
5. Schnittman, S.M., S.M. Denning, J.J. Greenhouse, J.S. Justement, M. Baseler, J. Kurtzberg, B.F. Haynes, and A.S. Fauci. 1990. Evidence for susceptibility of intrathymic T-cell precursors and their progeny carrying T-cell antigen receptor phenotypes TCR$\alpha\beta^+$ and TCR$\gamma\delta^+$ to human immunodeficiency virus infection: a mechanism for $CD4^+$ (T4) lymphocyte depletion. *Proc. Natl. Acad. Sci. USA*. 87:7727–7731.
6. Su, L., H. Kaneshima, M. Bonyhadi, S. Salimi, D. Kraft, L. Rabin, and J.M. McCune. 1995. HIV-1–induced thymocyte depletion is associated with indirect cytopathogenicity and infection of progenitor cells in vivo. *Immunity*. 2:25–36.
7. Rosenzweig, M., D.P. Clark, and G.N. Gaulton. 1993. Selective thymocyte depletion in neonatal HIV-1 thymic infection. *AIDS*. 7:1601–1605.
8. Stanley, S.K., J.M. McCune, H. Kaneshima, J.S. Justement, M. Sullivan, E. Boone, M. Baseler, J. Adelsberger, M. Bonyhadi, J. Orenstein, et al. 1993. Human immunodeficiency virus infection of the human thymus and disruption of the thymic microenvironment in the SCID-hu mouse. *J. Exp. Med*. 178:1151–1163.
9. Mitler, J.E., B.R. Levin, and R. Antia. 1996. T-cell homeostasis, competition and drift: AIDS as HIV-accelerated senescence of the immune repertoire. *J. Acquired Immune Defic. Syndr*. 12:233–248.
10. Wei, X., S.K. Ghosh, M.E. Taylor, V.A. Johnson, E.A. Emini, P. Deutsch, J.D. Lifson, S. Bonhoeffer, M.A. Nowak, B.H. Hahn, et al. 1995. Viral dynamics in human immunodeficiency virus type 1 infection. *Nature*. 373:117–122.
11. Mackall, C.L., T.A. Gleisher, M.R. Brown, M.P. Andrich, C.C. Chen, I.M. Feuerstein, M.E. Horowitz, I.T. Magrath, A.T. Shad, S.M. Steinberg, et al. 1995. Age, thymopoiesis, and CD4+ T-lymphocyte regeneration after intensive chemotherapy. *N. Engl. J. Med*. 332:143–149.
12. Ho, D., A.U. Neumann, A.S. Perelson, W. Chen, J.M. Leonard, and M. Markowitz. 1995. Rapid turnover of plasma virions and CD4 lymphocytes in HIV-1 infection. *Nature*. 373:123–126.
13. Mackall, C.L., V.C. Bare, L.A. Granger, S.O. Sharrow, J.A. Titus, and R.E. Gress. 1996. Thymic-independent T cell regeneration occurs via antigen-driven expansion of peripheral T cells resulting in a repertoire that is limited in diversity and prone to skewing. *J. Immunol*. 156:4609–4616.
14. Heitger, A., N. Neu, H. Kern, E.R. Panzer-Grumayer, H. Greinix, D. Nachbaur, D. Niederwieser, and F.M. Fink. 1997. Essential role of the thymus to reconstitute naive (CD45RA+) T-helper cells after human allogeneic bone marrow transplantation. *Blood*. 90:850–857.
15. Bonyhadi, M.L., L. Rabin, S. Salimi, D.A. Brown, J. Kosek, J.M. McCune, and H. Kanesha. 1993. HIV induces thymus depletion in vivo. *Nature*. 363:728–732.
16. Kaneshima, H., L. Su, M.L. Bonyhadi, R.I. Connor, D.D. Ho, and J.M. McCune. 1994. Rapid-high, syncytium-inducing isolates of human immunodeficiency virus type 1 induce cytopathicity in the human thymus of the SCID-hu mouse. *J. Virol*. 68:8188–8192.
17. Aldrovandi, G.M., G. Feuer, L. Gao, B. Jamieson, M. Kristeva, I.S.Y. Chen, and J.A. Zack. 1993. The SCID-hu

mouse as a model for HIV-1 infection. *Nature*. 363:732–736.
18. Namikawa, R., H. Kaneshima, M. Liberman, I.L. Weissman, and J.M. McCune. 1988. Infection of the SCID-hu mouse by HIV-1. *Science*. 242:1684–1686.
19. Desrosiers, R.C. 1990. The simian immunodeficiency viruses. *Annu. Rev. Immunol*. 8:557–578.
20. Watson, A., J. Ranchalis, B. Travis, J. McClure, W. Sutton, P.R. Johnson, S.L. Hu, and N.L. Haigwood. 1997. Plasma viremia in macaques infected with simian immunodeficiency virus: plasma viral load early in infection predicts survival. *J. Virol*. 71:284–290.
21. Hirsch, V.M., T.R. Fuerst, G. Sutter, M.W. Carroll, L.C. Yang, S. Goldstein, M. Piatak, W.R. Elkins, W.G. Alvord, D.C. Montefiori, et al. 1996. Patterns of viral replication correlate with outcome in simian immunodeficiency virus (SIV)-infected macaques: effect of prior immunization with a trivalent SIV vaccine in modified vaccinia virus Ankara. *J. Virol*. 70:3741–3752.
22. Kestler, H., T. Kodama, D. Ringler, M. Marthas, N. Pedersen, A. Lackner, D. Regier, P. Sehgal, M. Daniel, N. King, and R. Desrosiers. 1990. Induction of AIDS in rhesus monkeys by molecularly cloned simian immunodeficiency virus. *Science*. 248:1109–1112.
23. Kestler, H.W., D.J. Ringler, K. Mori, D.L. Panicali, P.K. Sehgal, M.D. Daniel, and R.C. Desrosiers. 1991. Importance of the *nef* gene for maintenance of high virus loads and for development of AIDS. *Cell*. 65:651–662.
24. Gibbs, J.S., A.A. Lackner, S.M. Lang, M.A. Simon, P.K. Sehgal, M.D. Daniel, and R.C. Desrosiers. 1995. Progression to AIDS in the absence of a gene for *vpr* or *vpx*. *J. Virol*. 69:2378–2383.
25. Daniel, M.D., Y. Li, Y.M. Naidu, P.J. Durda, D.K. Schmidt, C.D. Finger, D.P. Silva, J.J. MacKey, H.W. Kestler, P.K. Sehgal, et al. 1988. Simian immunodeficiency viruses from African green monkeys. *J. Virol*. 62:4123–4128.
26. Kawai, T., J. Wong, J. MacLean, A.B. Cosimi, and S. Wee. 1994. Characterization of a monoclonal antibody recognizing the cynomolgus monkey CD3 antigen. *Transplant. Proc*. 26: 1845–1846.
27. Ilyinskii, P.O., M.D. Daniel, M.A. Simon, A.A. Lackner, and R.C. Desrosiers. 1994. The role of upstream U3 sequences in the pathogenesis of SIV-induced AIDS in rhesus monkeys. *J. Virol*. 68:5933–5944.
28. Horvath, C.J., R.D. Hunt, M.A. Simon, P.K. Sehgal, and D.J. Ringler. 1993. An immunohistologic study of granulomatous inflammation in SIV-infected rhesus monkeys. *J. Leukocyte Biol*. 53:532–540.
29. Lackner, A.A., M. Schiødt, G.C. Armitage, P.F. Moore, R.J. Munn, P.A. Marx, M.B. Gardner, and L.J. Lowenstine. 1989. Mucosal epithelial cells and Langerhans cells are targets for infection by the immunosuppressive type D simian AIDS retrovirus serotype 1. *J. Med. Primatol*. 18:195–207.
30. Ringler, D.J., D.G. Walsh, L.V. Chalifoux, J.J. MacKey, M.D. Daniel, R.C. Desrosiers, N.W. King, and W.W. Hancock. 1990. Soluble and membrane-associated interleukin 2 receptor-alpha expression in rhesus monkeys infected with simian immunodeficiency virus. *Lab. Invest*. 62:435–443.
31. Sasseville, V.G., Z. Du, L.V. Chalifoux, D.R. Pauley, H.L. Young, P.K. Sehgal, R.C. Desrosiers, and A.A. Lackner. 1996. Induction of lymphocyte proliferation and severe gastrointestinal disease in macaques by a nef gene variant of SIVmac239. *Am. J. Pathol*. 149:163–176.
32. Keshgeian, A.A., and A. Cnaan. 1995. Proliferation markers in breast carcinoma: mitotic figure count, S-phase fraction, proliferating cell nuclear antigen, Ki-67 and MIB-1. *Am. J. Clin. Pathol*. 104:42–49.
33. Kelleher, L., H.M. Magee, and P.A. Dervan. 1994. Evaluation of cell-proliferation antibodies reactive in paraffin sections. *Appl. Immunohistochem*. 2:164–170.
34. Barbareschi, M., S. Girlando, F.M. Mauri, S. Forti, C. Eccher, F.A. Mauri, R. Togni, P.D. Palma, and C. Doglioni. 1994. Quantitative growth fraction evaluation with MIB1 and Ki67 antibodies in breast carcinomas. *Am. J. Clin. Pathol*. 102:171–175.
35. Landberg, G., E.M. Tan, and G. Roos. 1990. Flow cytometric multiparameter analysis of proliferating cell nuclear antigen/cyclin and Ki-67 antigen: a new view of the cell cycle. *Exp. Cell. Res*. 187:111–118.
36. Sarli, G., C. Benazzi, R. Preziosi, and P.S. Marcato. 1994. Proliferative activity assessed by anti-PCNA and Ki67 monoclonal antibodies in canine testicular tumours. *J. Comp. Path*. 110:357–368.
37. Gavrieli, Y., Y. Sherman, and S.A. Ben-Sasson. 1992. Identification of programmed cell death in situ via specific labeling of nuclear DNA fragmentation. *J. Cell Biol*. 119:493–501.
38. Tenner-Racz, K., P. Racz, C. Thomé, C.G. Meyer, P.J. Anderson, S.F. Schlossman, and N.L. Letvin. 1993. Cytotoxic effector cell granules recognized by the monoclonal antibody TIA-1 are present in CD8+ lymphocytes in lymph nodes of human immunodeficiency virus-1–infected patients. *Am. J. Pathol*. 142:1750–1758.
39. Meehan, S.M., R.T. McCluskey, M. Pascual, F.L. Preffer, P. Anderson, S.F. Schlossman, and R.B. Colvin. 1997. Cytotoxicity and apoptosis in human renal allografts: Identification, distribution, and quantitation of cells with a cytotoxic granule protein GMP-17 (TIA-1) and cells with fragmented nuclear DNA. *Lab. Invest*. 76:639–649.
40. Lackner, A.A., P. Vogel, R.A. Ramos, J.D. Kluge, and M. Marthas. 1994. Early events in tissues during infection with pathogenic (SIVmac239) and nonpathogenic (SIVmac1A11) molecular clones of simian immunodeficiency virus. *Am. J. Pathol*. 145:428–439.
41. Zhang, J., L.N. Martin, E.A. Watson, R.C. Montelaro, M. West, L. Epstein, and M. Murphey-Corb. 1988. Simian immunodeficiency virus/delta-induced immunodeficiency disease in rhesus monkeys: relation of antibody response and antigenemia. *J. Infect. Dis*. 158:1277–1286.
42. Daniel, M.D., F. Kirchoff, S.C. Czajak, P.K. Sehgal, and R.C. Desrosiers. 1992. Protective effects of a live attenuated SIV vaccine with a deletion in the *nef* gene. *Science*. 258: 1938–1941.
43. Baskin, G.B., M. Murphey-Corb, L.N. Martin, B. Davison-Fairburn, F.-S. Hu, and D. Kuebler. 1991. Thymus in simian immunodeficiency virus–infected rhesus monkeys. *Lab. Invest*. 65:400–407.
44. Terstappen, L.W., S. Huang, and L.J. Picker. 1992. Flow cytometric assessment of human T-cell differentiation in thymus and bone marrow. *Blood*. 79:666–677.
45. Kourtis, A.P., C. Ibegbu, A.J. Nahmias, F.K. Lee, W.S. Clark, M.K. Sawyer, and S. Nesheim. 1996. Early progression of disease in HIV-infected infants with thymic dysfunction. *N. Engl. J. Med*. 335:1431–1436.
46. Connors, M., J.A. Kovacs, S. Krevat, J.C. Gea-Banacloche, M.C. Sneller, M. Flanigan, J.A. Metcalf, R.E. Walker, J. Falloon, M. Baseler, et al. 1997. HIV induces changes in CD4+ T-cell phenotype and depletions within the CD4+ T-cell

repertoire that are not immediately restored by antiviral or immune-based therapies. *Nat. Med.* 3:533–540.
47. Autran, B., G. Carcelain, T.S. Li, C. Blanc, D. Mathez, R. Tubiana, C. Katlama, P. Debré, and J. Leibowitch. 1997. Positive effects of combined antiretroviral therapy on CD4+ T cell homeostasis and function in advanced HIV disease. *Science*. 277:112–116.
48. Jacobson, M.A., F. Kramer, P.R. Pavan, S. Owens, R. Pollard, and N.A.P. Team. 1997. Failure of highly active antiretroviral therapy (HAART) to prevent CMV retinitis despite marked CD4 count increase. *Proceedings of the 4th Conference on Retroviruses and Opportunistic Infections*. 129:353. (Abstr.)
49. Gilquin, J., C. Piketty, V. Thomas, G. Gonzales-Canali, and M.D. Kazatchkine. 1997. Acute CMV infection in AIDS patients receiving combination therapy including protease inhibitors. *Proceedings of the 4th Conference on Retroviruses and Opportunistic Infections*. 129:354 (Abstr.)
50. Rosenzweig, M., M. DeMaria, D.M. Harper, S. Freidrich, R.K. Jain, and R.P. Johnson. 1998. Increased rates of $CD4^+$ and $CD8^+$ T lymphocyte turnover in simion immunodeficiency virus-infected macaques. *Proc. Natl. Acad. Sci. USA*. In press.
51. Du, Z.J., S.M. Lang, V.G. Sasseville, A.A. Lackner, P.O. Ilyinskii, M.D. Daniel, J.U. Jung, and R.C. Desrosiers. 1995. Identification of a nef allele that causes lymphocyte activation and acute disease in macaque monkeys. *Cell*. 82:665–674.